



## Dependence of offshore wind turbine fatigue loads on atmospheric stratification

Hansen, Kurt Schaldemose; Larsen, Gunner Chr.; Ott, Søren

*Published in:*  
Journal of Physics: Conference Series (Online)

*Link to article, DOI:*  
[10.1088/1742-6596/524/1/012165](https://doi.org/10.1088/1742-6596/524/1/012165)

*Publication date:*  
2014

*Document Version*  
Publisher's PDF, also known as Version of record

[Link back to DTU Orbit](#)

*Citation (APA):*  
Hansen, K. S., Larsen, G. C., & Ott, S. (2014). Dependence of offshore wind turbine fatigue loads on atmospheric stratification. *Journal of Physics: Conference Series (Online)*, 524(1), [012165].  
<https://doi.org/10.1088/1742-6596/524/1/012165>

---

### General rights

Copyright and moral rights for the publications made accessible in the public portal are retained by the authors and/or other copyright owners and it is a condition of accessing publications that users recognise and abide by the legal requirements associated with these rights.

- Users may download and print one copy of any publication from the public portal for the purpose of private study or research.
- You may not further distribute the material or use it for any profit-making activity or commercial gain
- You may freely distribute the URL identifying the publication in the public portal

If you believe that this document breaches copyright please contact us providing details, and we will remove access to the work immediately and investigate your claim.

## Dependence of offshore wind turbine fatigue loads on atmospheric stratification

This content has been downloaded from IOPscience. Please scroll down to see the full text.

2014 J. Phys.: Conf. Ser. 524 012165

(<http://iopscience.iop.org/1742-6596/524/1/012165>)

View [the table of contents for this issue](#), or go to the [journal homepage](#) for more

Download details:

IP Address: 192.38.90.17

This content was downloaded on 20/06/2014 at 10:31

Please note that [terms and conditions apply](#).

## Dependence of offshore wind turbine fatigue loads on atmospheric stratification

**K S Hansen<sup>1</sup>, G C Larsen and S Ott**

Department of Wind Energy, Technical University of Denmark  
Nils Koppels Allé, B403-DTU, DK-2800 Kgs.Lyngby, Denmark

E-mail: kuhan@dtu.dk

**Abstract.** The stratification of the atmospheric boundary layer (ABL) is classified in terms of the M-O length and subsequently used to determine the relationship between ABL stability and the fatigue loads of a wind turbine located inside an offshore wind farm. Recorded equivalent fatigue loads, representing blade-bending and tower bottom bending, are combined with the operational statistics from the instrumented wind turbine as well as with meteorological statistics defining the inflow conditions. Only a part of all possible inflow conditions are covered through the approximately 8200 hours of combined measurements. The fatigue polar has been determined for an (almost) complete 360° inflow sector for both load sensors, representing mean wind speeds below and above rated wind speed, respectively, with the inflow conditions classified into three different stratification regimes: unstable, neutral and stable conditions. In general, impact of ABL stratification is clearly seen on wake affected inflow cases for both blade and tower fatigue loads. However, the character of this dependence varies significantly with the type of inflow conditions – e.g. single wake inflow or multiple wake inflow.

### 1. Introduction

Grouping two or more wind turbines, results in a loss of energy production and reduced fatigue life when the turbines operate in the wake. The increased fatigue life consumption primarily depends on inter turbine spacing, turbulence intensity, turbulence structure, atmospheric stratification and wind speed. Since the wake operation can result in a significant increase in fatigue life consumption compared to free inflow conditions, it is extremely important to include the wake cases in the wind farm optimization process. While previous analysis of the wind turbine loading in the Horns Rev 1 wind farm have been focusing on comparing the wind turbine loading in free and disturbed inflow sectors [2] under neutral conditions, the purpose of the present paper is to investigate the impact from atmospheric stability on fatigue loading of offshore wind farm turbines. For this purpose full-scale measurements, from an 80m/2MW V80 wind turbine located inside the Horns Rev wind farm, have been analyzed. A previous related analysis [1] has focused on the impact from ABL stratification on annual energy production of this wind farm. The Horns Rev wind farm represents a regular layout with flat and uncomplicated inflow conditions. This is a big advantage for the “tractability” of various effects in an analysis as the present, and contrary to the situation for wind farms located in e.g. pastoral or complex terrain where flow features typically are much more complicated due to local terrain effects and local thermal effects

<sup>1</sup> To whom any correspondence should be addressed.



A new robust method [1], based on the Monin-Obukhov theory, is used to classify the site ABL stability characteristics as based on site meteorological recordings from two meteorological towers located outside the wind farm. More specific inflow characteristics, like mean wind speed and mean wind direction, are obtained using wind turbine SCADA data.

## 2. Wind farm and wind turbine measurements

### 2.1. Wind farm

The Horns Rev offshore wind farm has a capacity of 160 MW and is located 14 km from the west coast of Denmark. The wind farm features are described in detail in [1]. The wind farm comprises 80 wind turbines, which are arranged in a regular array of 8 by 10 turbines, see Figure 1. The naming convention in this article is that the western NS row includes turbines 1 – 8 and the next NS row includes turbines 11-18. Two 70m mast, located east of the wind farm, have been used to quantify the site ABL stability conditions.

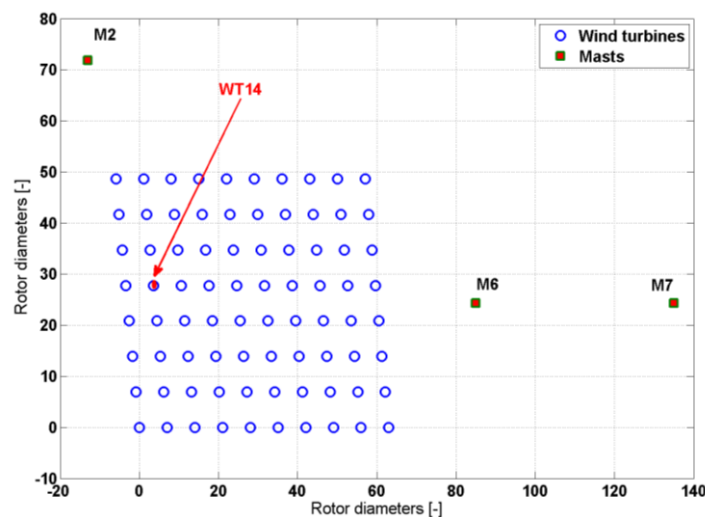


**Figure 1:** Layout of Horns Rev wind farm including the location of wind turbine WT14.

The wind farm turbines are VESTAS V80 turbines, which are 2MW pitch controlled, variable speed wind turbines with a diameter of 80m and 70m hub height. The wind turbine operation is basically characterized by a combined variable rotor speed below rated power and variable pitch angle for the mean wind speed regime corresponding to rated power and above.

The measurement systems at Horns Rev includes several subsystems, which have been in operation for several years; unfortunately not all instruments have been calibrated and/or quality controlled regularly. However, a quality control procedure has been implemented based on the guidelines developed as part of the UPWIND project [7].

### 2.2. Meteorological data

The Horns Rev database includes 10 minute statistics of wind speeds, directions and other meteorological parameters both from mast M2 and the two ‘wake masts’ located 2km and 6km to the east of the array, respectively (cf. Figure 1). Before being included in the database, these data have passed a quality screening.

The undisturbed wind farm inflow, characterized with wind speed and wind direction is only measured for an easterly sector, Figure 1. Instead it has been necessary to derive these signals from the wind turbines while these signals are essential for the planned analysis.

The ambient wind direction has been derived based on the wind turbine nacelle position from pairs of undisturbed wind turbines assuming no yaw misalignment. This derived wind direction has been calibrated based on identified maximum power deficits related to different pairs of wind turbines representing 8 distinct flow directions, in which the positions of the upstream turbine varied between 7D and 10D. The eight ambient flow directions used for this calibration are: 41°, 90°, 132°, 173°, 221°, 270°, 312° and 353°. As a result, the derived site wind direction signal thus represents the complete 0 – 360° inflow sector to the wind farm.

The inflow wind field to wind turbine WT14 depends highly on whether the inflow is undisturbed or disturbed to a given level by upstream located turbines (e.g. WT14 is operating partly in the wake of between 1 and 8 wind turbines depending on the mean wind direction). The wind speed measured on top of the nacelle correlates well with the ambient inflow wind speed up to approximately 11 m/s for an undisturbed flow sector. Beyond the rated output wind speed (i.e. approximately 11 m/s) the rotor thrust and thereby the rotor induction decreases, which in turn results in a decreased correlation between the inflow wind speed and the nacelle measured wind speed. Based on these considerations, the nacelle wind speed was selected as the “local” mean wind speed in the mean wind speed regime up to approximately 11 m/s.

### 2.3. SCADA data

The SCADA data from Horns Rev consists of 10-minute statistical data for each of the 80 wind turbines and these data includes active power and nacelle wind speed. Furthermore the operational conditions of the wind turbine are categorized with the pitch angle, rotor speed and yaw position.

### 2.4. Structural data

The structural measurements have been recorded on one turbine only, WT14, which is located in the second NS row - as indicated in Figure 1. The measurements have been recorded by DONG (formerly ELSAM) and VESTAS Wind Systems during the period 2005 - 2007 with a sampling frequency of 20 Hz. Due to quality problems the data has been filtered and scaled afterwards by DONG [5]. Moreover, only one pair of blade root moments (i.e. edgewise as well as flapwise moments) together with the tower base bending moment sensors have been usable for the wake load studies. This is due to defective sensors or irreversible miscalibrations.

The structural measurements were recorded in the period 2005.08 – 2007.06, but only a limited amount of time series passed the qualification. The dataset includes structural measurements only, and unfortunately no information about the wind turbine operational conditions, as e.g. power production, pitch setting or rotor speeds, are available. Moreover, due to the poor synchronization between the structural and the SCADA dataset, the edgewise signal has been used to identify and filter for undesirable events like idling and start/stop sequences. Finally, periodic problems and spikes associated with the rotor located strain gauge amplifier were circumvented by suitable filtering.

In total, four structural signals have been used in this analysis:

- i) Flapwise blade-bending moment ( $M_{xA1}$ ): Blade A at  $r = 1.7$  m;
- ii) Edgewise blade-bending moment ( $M_{yA1}$ ): Blade A, at  $r = 1.7$  m;
- iii) Tower bending NS ( $M_{ns5}$ ) at  $h = 13$  m above mean sea level (AMSL);
- iv) Tower bending EW ( $M_{ew5}$ ) at  $h = 13$  m AMSL.

Inspection of the dataset has revealed that the tower bottom signals in general seem to be of higher quality than the rotor signals. To improve the quality of both data sets these have been re-calibrated as described below.

### 2.5. Synchronization

Unfortunately the SCADA data, which has been used in a previous flow analysis [4], cannot be directly synchronized with the structural load signals due a lack of overlapping signals. Therefore, the synchronization between SCADA data and structural measurements is only assured to be within a time

span of  $\pm 600$  seconds. Furthermore, wind turbine grid connection (i.e. that the turbine is in normal operation) can only be identified from analysis of the standard deviation of the edgewise blade-bending moment, as no power output information is available. The lack of synchronization might include events (e.g. idling, start, stop or emergency stop) with increased or decreased loading compared to 100% grid connected power production, and therefore in turn increases the uncertainty of the reported equivalent loads.

### 2.6. Rotor loads

The flapwise blade root moment, which is the out-of-rotor bending moment in the blade root, will be used in the succeeding rotor load analysis.

A recalibration, based on gravity blade loading, recorded during low wind idling has been performed for both flap wise and edgewise rotor signals to ensure an acceptable signal quality. Signal MyA1 has only been used for validation of amplifier quality and the operational condition of the wind turbine. Using a filtering procedure based on an analysis of the quality of the strain gauge signals, a considerable amount of these data was rejected due to noise issues, thus reducing the dataset for the flapwise blade-bending moments to approximately 2200 hours. The flapwise gain re-calibration was done taking advantage of gravity loading during 5 periods, where the turbine was idling below cut-in wind speed. The statistics representing the flapwise loading are stored as 10 minute mean values and equivalent fatigue load values assuming a Wöhler material exponent of  $m = 10$ . A detailed definition of the S-N or Wöhler curve is given in [11].

### 2.7. Tower loads

A conventional recalibration, based on gravity dictated nacelle loading, using tower bending moments recorded during low wind cable untwisting (i.e. rotor yawing) has been performed for both tower bottom signals. Subsequently, both tower bending moment signals have been filtered to eliminate outliers and persistence e.g. where the signal demonstrated very low variation during operation. During this filtering the dataset was reduced to approximately 5000 hours.

The maximum tower bottom bending moment,  $M_t$ , has been derived from the Mns5 and Mew5 recordings according to (1) for each time step,  $i$ , where  $i$  denotes the  $i$ 'th scan performed with a scan frequency of 20Hz. Using (1) is a conservative approach instead of using the correct inflow angle, which is not available due to the above mentioned synchronization problem, but the difference is marginal.

$$t_i = \sqrt{Mns5_i^2 + Mew5_i^2} \quad (1)$$

The  $M_t$  signal are stored in the database both as 10 minute mean values and as equivalent fatigue equivalent load values assuming a Wöhler material exponent  $m = 6$ . Although the phase angle of the tower bottom bending moment,  $\mathbf{M}_b = (Mns5, Mew5)$ , with magnitude  $M_t$  will vary moderately during a 10-minute measuring sequence,  $\mathbf{M}_b$  predominantly reflects the tower tilt loading, and  $M_t$  will therefore in the following be referred to as the tower tilt moment.

## 3. Data analysis

### 3.1. Classification of the atmospheric stability

Atmospheric stratification is traditionally characterized in terms of the Monin-Obukhov (MO) length  $L$  [9], where  $1/L$  by definition is equal to

$$1/L = (g \theta_*) / (\kappa T_s u_*^2) \quad (2)$$

In the present analysis  $L$  is determined accordingly and subsequently included in the measurement database as an additional derived signal; this enables a straight forward merger of this “channel” with the other wind farm measurement channels.

The calculation of  $L$  is performed using the AMOK code as based on equations presented in [1]. The input to AMOK is three measured signals from mast M7:

- Wind speed; measured 20m above mean sea surface level;
- Air temperature; measured 28m above mean sea surface level;
- Sea temperature; measured 3m below above mean sea surface level.

Depending on the ambient mean wind direction, the derived MO length is therefore based on a mix of observations recorded both within and outside the *wind farm* wake. However, based on a validation check between M2 and M7 observations (cf. Figure 1) it was concluded, that the potential impact from the wind farm wake only affects the stability distribution marginally. This is probably due to the large separation between the wind farm and M7.

An often used stability classification system for the ABL has been proposed Gryning et al. [8]. This system defines 7 stability classes ranging from very unstable to very stable. However, to ensure a sufficient number of 10-minute observations in each class with the available data material, it was found appropriate to collapse the original seven classes into a more coarse classification consisting of three classes only. These were obtained by merging the very unstable and the unstable classes of Gryning into one unstable class; by merging the original near unstable, neutral and near stable classes into a neutral class; and by merging the very stable and the stable classes into one stable class. The resulting three classes defined for the present investigation is shown in Table 1.

**Table 1:** Definition of stratification used in present analysis for hub height  $z=70\text{m}$

Stability class	MO length [m]	$z/L$ [-]
Unstable	$-200 \leq L < -50$	$-1.4 < z/L \leq -0.35$
Neutral	$ L  > 200$	$ z/L  < 0.35$
Stable	$10 < L \leq 200$	$0.35 \leq z/L < 7.00$

The relative distributions on the three stability classes are shown in Figures 2 and 3 for the investigated mean wind speed intervals (i.e. 8 – 10 m/s and 10 – 15m/s, respectively). The distribution demonstrates a high occurrence of stable stratification, especially for westerly winds. However, the distribution probably also depends on the season [10] and we don't know how the recording times are distributed over the year.

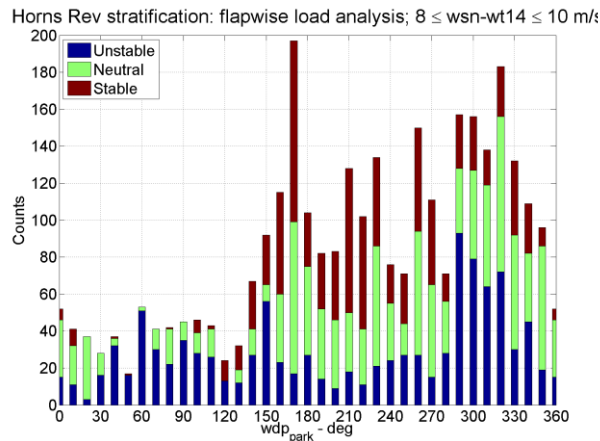


**Figure 2:** Polar stratification for 360 degree inflow, 8 - 10 m/s.

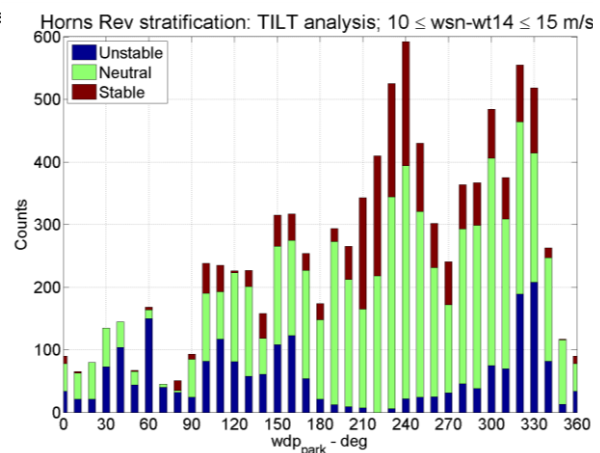


**Figure 3:** Polar stratification for 360 degree inflow, 10 - 15 m/s.

### 3.2. Definition of suitable mean wind speed bins

Having defined suitable bins for the stability classification, we now consider definition of suitable bins for the mean wind speed. As with the stability classification, selection of suitable bins is always a compromise between small bin widths and sufficiently well populated bins. With a focus on wind turbine fatigue loads the basic challenge is that the fatigue loads may depend significantly on the inflow wind speed. For not too densely populated mean wind speed bins, there is a risk that the distributions of inflow mean wind speeds, within these bins, are different for different stability bins. This is unfortunate, because it may hinder separation of mean wind speed effects from effects associated with atmospheric stability. The way to circumvent this problem is to define mean wind speed bins, within which the fatigue loading in question is only moderately dependent on the wind speed.

The present analysis concerns blade flap fatigue loads and tower bottom fatigue loading, and for each of these load categories the dependence of fatigue loading, expressed in terms of fatigue equivalent moments, with the inflow mean wind speed has been investigated both for free and for wake affected inflow conditions, respectively. The reason for the split in free and waked conditions is that the inflow turbulence conditions, which is the main driver of the investigated fatigue loading, depends significantly on the turbine being in waked conditions or not. The results are shown in Figures 4-5.

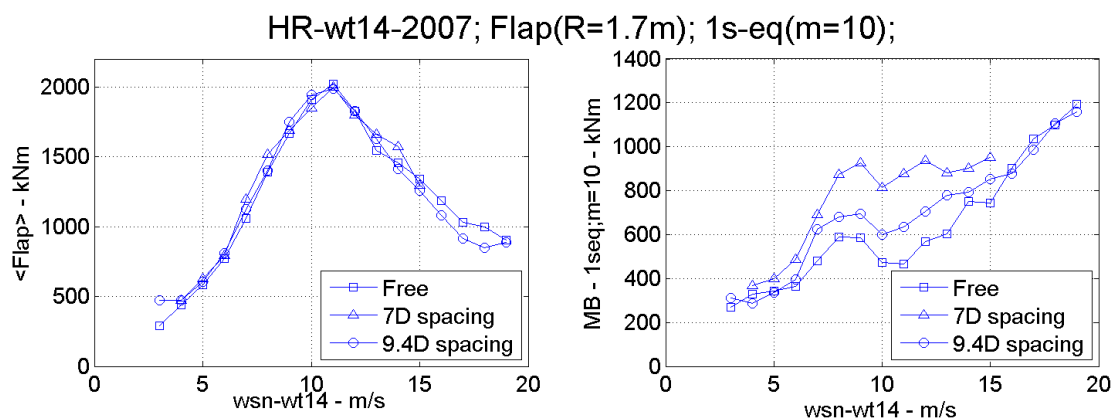


**Figure 4:** Mean flap loads (left) and flap equivalent moments (right).



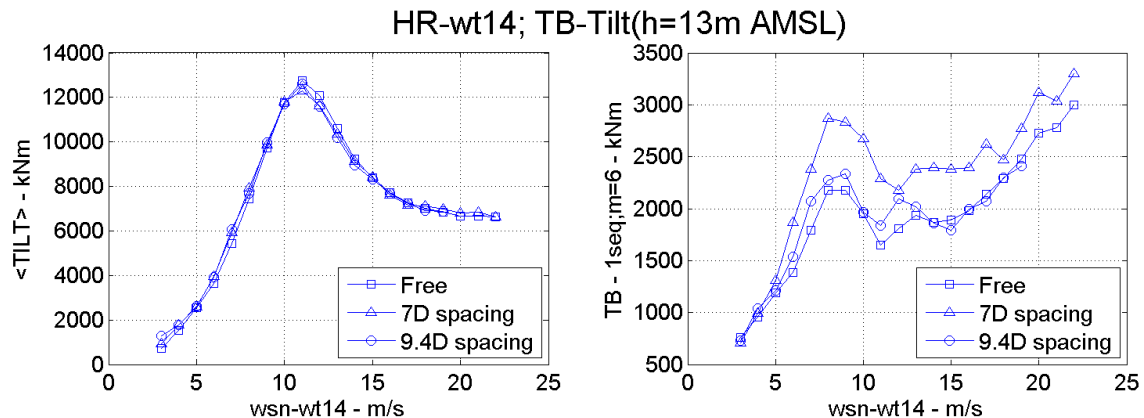


**Figure 5:** Mean tilt loads (left) and tilt equivalent moments (right).

Referring to Figures 4-5, the equivalent tower bending moment is seen to be only moderately dependent on wind speed in the interval 10-15 m/s, and the same holds for the equivalent flapwise blade-bending moment for wind speeds in the interval 8-10 m/s. An additional concern is that the gravitational component of the flapwise blade-bending moment depends on the pitch angle, but fortunately the pitch angle is constant up to 11 m/s. These intervals were therefore selected for the subsequent analysis of the influence of stability in order to reduce wind speed induced bias.

The size of the dataset covering the wind speed interval [8m/s ; 10m/s] amounts to approximately 555 hours, whereas the size of the data set covering to the mean wind speed bin [10m/s ; 15m/s] is approximately 1590 hours.

## 4. Results and discussion

### 4.1. Rotor loads

The rotor loads have been extracted as function of park wind direction for the wind speed ( $U$ ) interval defined in the previous chapter for the three different stratification groups defined in Table 1. The results are plotted as a polar in Figure 6, where the effect of upstream emitted wakes is clearly visible at distinct wind directions.

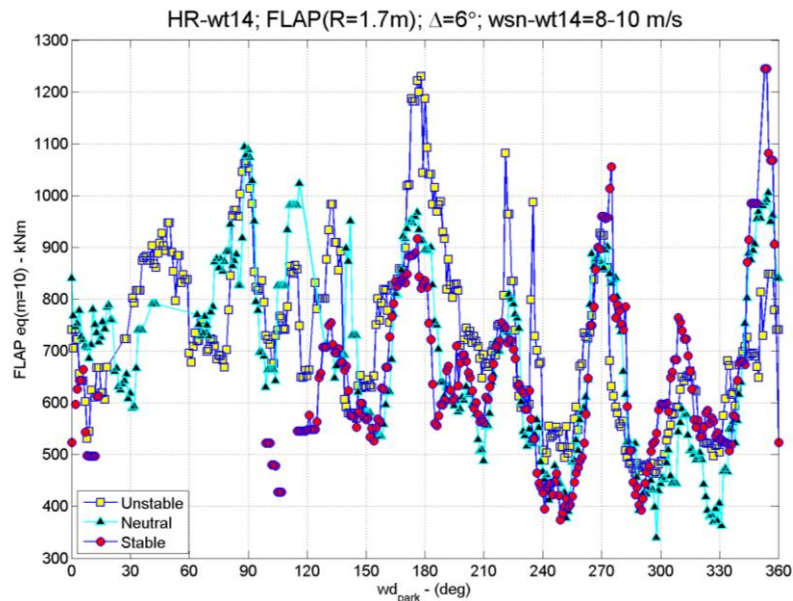


**Figure 6:** Polar flap equivalent moment;  $U \in [8 ; 10 \text{ m/s}]$ .

The rotor fatigue loads clearly display dependence with the atmospheric stratification, but the character of this dependence seems to be highly affected by the particular type of inflow conditions – i.e. free inflow, single wake inflow or multiple wake inflow. Moreover, a dependence on turbine spacing can be identified for the wake affected inflow conditions. As expected, the rotor fatigue loading increases with decreasing turbine inter spacing. For single wake conditions this is seen by comparing the rotor loads corresponding to inflow directions  $270^\circ$  (7D),  $221^\circ$  (9.4D) and  $312^\circ$  (10.4D). For multiple wake conditions this is seen by comparing the rotor loads corresponding to inflow directions  $173^\circ$  (7D) and  $132^\circ$  (10.4D). In the following the  $270^\circ$  single wake case and the  $173^\circ$  multiple wake case will be analysed in more detail.

To reduce scatter a  $6^\circ$  sliding averaging filtering procedure was applied on the single wake data, and each window was furthermore required to represent at least 30 minutes of measurements (i.e. at least 3 10 minute time series). Error bars were computed with magnitudes equal to the standard deviation of each window mean value, and the results for the defined ABL stability classes are shown in Figure 7.

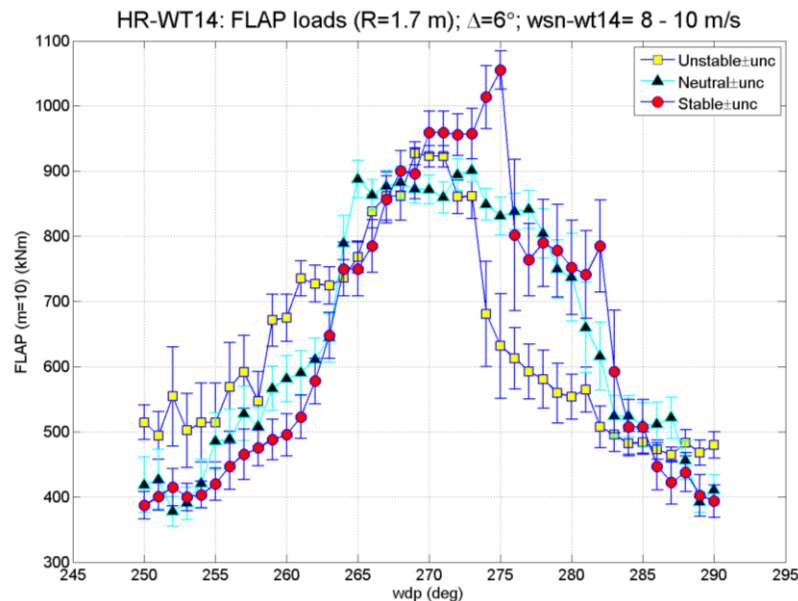


**Figure 7:** Flapwise equivalent as function of ambient wind direction;  
 $U \in [8 ; 10 \text{ m/s}]$ ; 7 D spacing.

The rotor loads are observed to increase up to approximately 150% compared to free inflow conditions. Stable stratification is seen to have the most significant effect on the flapwise fatigue loading in the direction regime in the vicinity of  $270^\circ$ , where full and half wake situations are predominant. In stable stratification the wake meandering [12] is moderate, and a considerable fatigue load increase in this regime is therefore expected due to dynamic loads caused by blades moving in and out of a “quasi-static” wake. For neutral and unstable conditions the wake meandering is more intense, and the blade flapwise fatigue loading is resulting from a mix of blades moving in and out of the wake, and a more dynamically active wake sweeping across the rotor plane. However, the lack of symmetric patterns in the measurements can only be explained by a large statistical uncertainty, which does not allow us to draw firm conclusions.

In the direction regimes far from the centre wind direction, i.e. direction regimes close to  $250^\circ$  or  $290^\circ$ , stable stratification results in the lowest fatigue loads, presumable because the emitted wakes never or seldom reach these directions due to moderate wake meandering. By analogy with this interpretation, unstable stratification results in the largest fatigue loads in this regime, and neutral stratification results in fatigue load levels exceeding the fatigue loads associated with stable stratification.

As for the multiple wake case characterized by a centre wind direction of  $173^\circ$  a data processing analogous to the one described for the single wake case was performed. The result is shown in Figure 8. With reference to Figure 1, the investigated turbine is seen to operate in the wakes of four upstream turbines with an inter turbine spacing of 7D. An impact of ABL stability on the fatigue loads is observed, with unstable stratification giving rise to the largest fatigue load increase for wind directions larger than approximately  $170^\circ$ , where also the stable stratification is giving rise to the smallest fatigue load increase. For wind directions less than  $170^\circ$  the ranking is different. Note also the difference from the  $90^\circ$  peak (in Figure 6), where there is little difference between the three stratifications with neutral stratification yielding smaller values in some cases.

Again the peak showed in Figure 8 demonstrates a great deal of asymmetry around  $173^\circ$ . The farm layout is slightly skewed, and WT14 occupies a non-symmetric position, but it seems unlikely that this could explain the large asymmetry seen in Figure 7. Compared to the flapwise fatigue load level for free undisturbed inflow with a mean wind speed of 10m/s, the wake affected fatigue loads are increased in the range 85 - 160% depending on ABL stratification conditions. The fatigue load level associated with unstable stratification is significantly higher than observed for the single wake case.

Further, the regime with significantly increased load levels for stable stratification is wider that observed for the single wake case, reflecting the increased variability of the wake position. This is due to increased meandering, which in turn is associated with increased downstream distance (i.e. here ranging from 7D to 28D).

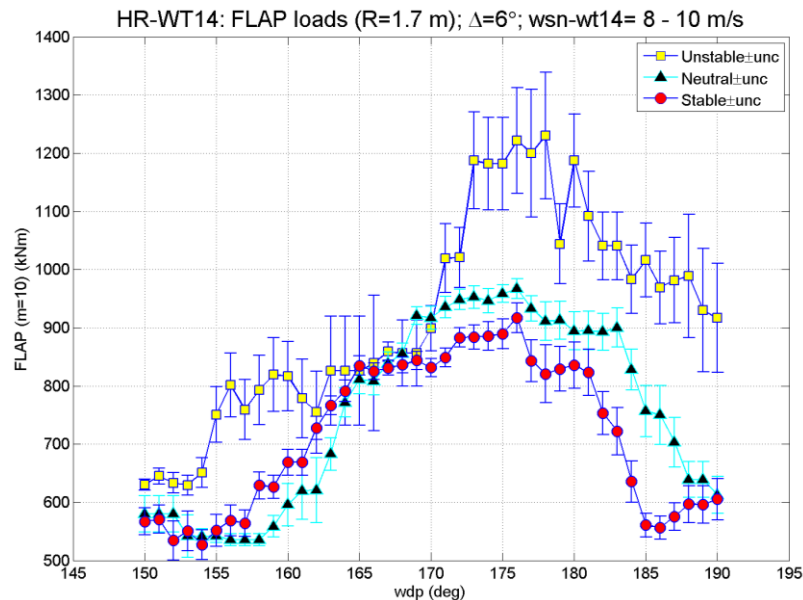


**Figure 8:** Flapwise equivalent as function of ambient wind direction;  $U \in [8 ; 10 \text{ m/s}]$ ; 7-28 D spacing.

#### 4.2. Tower loads

In analogy with blade flapwise fatigue loads, tower bottom tilt fatigue loads have been extracted for the wind speed interval defined in the previous chapter and for the three district stratification groups defined in Table 1. The data processing is as described for the flapwise fatigue loads, and the resulting polar plot is shown in Figure 9.

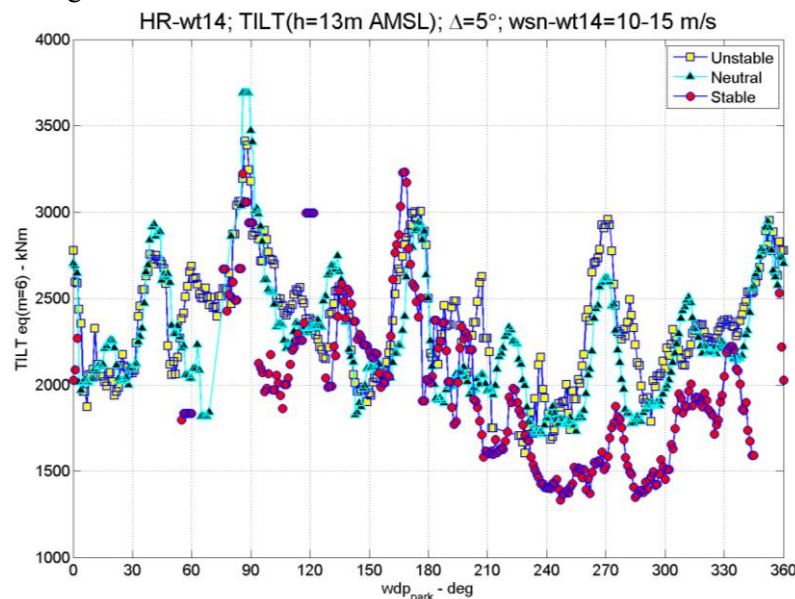


**Figure 9:** Polar tower tilt equivalent moment;  $U \in [10 ; 15 \text{ m/s}]$ .

The tower tilt fatigue load level depends on ABL stratification, but as with the flapwise blade loading the character of this dependence seems to be highly affected by the particular type of inflow conditions

(i.e. free inflow, various types of wake affected inflow and associated turbine spacing(s)). For single wake conditions this is seen by comparing the tower loads corresponding to inflow directions  $270^\circ$  (7D),  $221^\circ$  (9.4D) and  $312^\circ$  (10.4D), respectively. For multiple wake conditions this is seen by comparing the tower loads corresponding to inflow directions  $173^\circ$  (7D) and  $132^\circ$  (10.4D), respectively. As expected, the tower tilt fatigue loading increases with decreasing turbine inter spacing. As with the blade flapwise loads the  $270^\circ$  single wake case and the  $173^\circ$  multiple wake case will be analyzed in more detail.

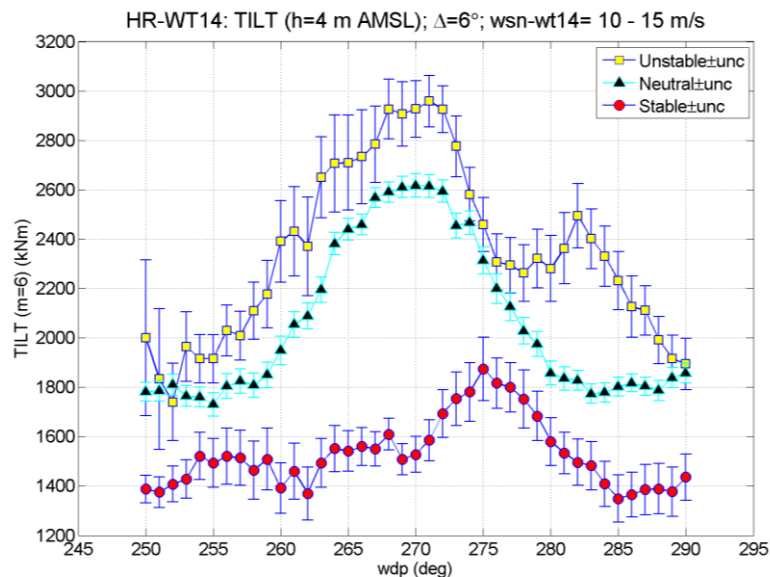


**Figure 10:** Tower bottom tilt equivalent moment;  
 $U \in [10 ; 15 \text{ m/s}]$ ; 7D spacing.

Significant impact from ABL stability conditions is observed on the fore-aft tower bottom fatigue loading on Figure 10 and the measurements seem less scattered than the corresponding flapwise blade-bending moments. This is in agreement with the initial observation – i.e. that the tower bottom signals “in general seem to be of higher quality than the rotor signals”. Note that the error bars indicate data scatter, not systematic errors. The ‘additional’ peak in the unstable data around  $282^\circ$  must be a statistical fluctuation because there are no upwind objects present that can modify the inflow conditions and thereby explain this type of load behaviour. The peak emphasizes the large uncertainty given in dataset caused by poor synchronization. The Coriolis force is most dominant for stable stratification and can be expected to shift the stable data points to the right in the plot. However, the peak of the stable data is just slightly more pronounced than the ‘extra’ peak, and the observed shift may therefore not be significant. The two other peaks single wake situations around  $222^\circ$  and  $312^\circ$  exhibit the same tendencies with significantly less impact for stable stratification than for neutral stratification (there are almost no unstable data at  $222^\circ$ ).

As seen from Figure 10, unstable ABL stratification seems to have the most significant impact on the tower fatigue loading, whereas stable stratification affects the tower fatigue loading the least for this single wake case. This is in agreement with the wake meandering being modest for stable conditions and somewhat more violent for the unstable conditions. Contrary to the rotor loading, where the fatigue loading is the result of conventional turbulence superimposed by both wake meandering and rotor rotation causing the blades to pass in and out of a wake if the wake is located fully or partially in the rotor plane, the fluctuation in tower loading are dictated only by conventional turbulence and wake meandering and therefore directly related to the wake meandering intensity.

The tower fatigue results for the multiple wake case, characterized by a centre wind direction of  $173^\circ$ , are shown in Figure 11.

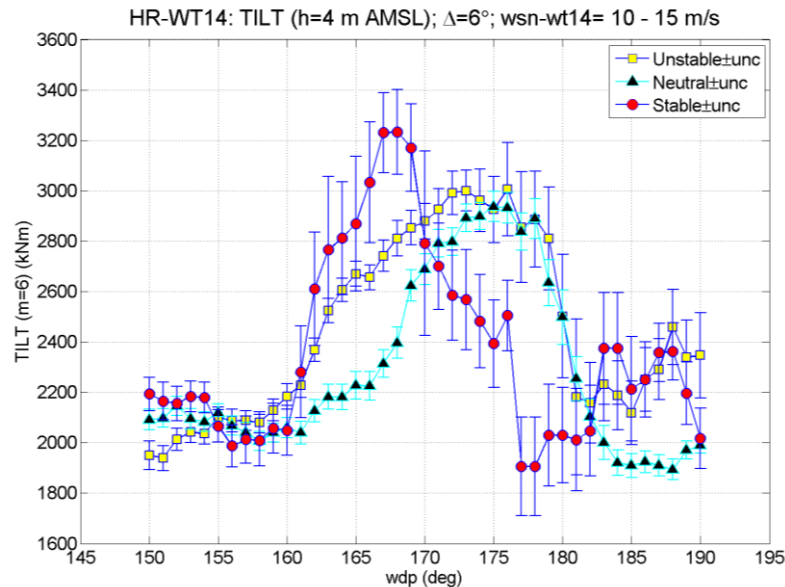


**Figure 11:** Tower bottom tilt equivalent moment,  
U: [10 ; 15 m/s] at 4 x 7 D spacing.

Again, an impact from ABL stability is observed. As with the blade fatigue loading the interpretation of the multiple wake case is less obvious than for the single wake case. The wake generated fatigue load increase is roughly comparable for all 3 stability classes, however, with a tendency of the width of the peak being smallest for stable stratification and largest for the unstable stratification. This is again in agreement with the wake meandering intensity/activity in general being least for stable stratification and largest for unstable stratification.

## 5. Conclusion

Analyses of full-scale load measurements on WT14 in the Horns Rev wind farm have been performed. Three stability classes – unstable, neutral and stable ABL stratification – have been considered with the aim of investigating the dependence of blade and tower fatigue loading on atmospheric stratification.

For all ABL stability classes, the effect of upstream emitted wakes is clearly visible at distinct wind directions for both blade and tower fatigue loads, and further an impact of ABL stratification is clearly seen on wake affected inflow cases. However, the character of this dependence varies significantly with the type of inflow conditions – e.g. single wake inflow or multiple wake inflow.

Stable stratification is seen to have the most significant effect on the flapwise fatigue loading for the investigated single wake case. Unstable stratification is seen to have the most significant effect on the flapwise fatigue loading for the investigated multiple wake case.

Concerning the single wake for-aft tower bottom fatigue loading, unstable ABL stratification has by far the most significant impact, whereas stable stratification affects the tower fatigue loading the least. This is contrary to the multiple wake case, where the wake generated fatigue load increase is roughly of the same order of magnitude for all 3 stability classes.



## 6. Acknowledgement

Research is funded by EUDP: Grant 64010-0462 “Impact of atmospheric stability conditions on wind farm loading and production”. We furthermore acknowledge Vattenfall AB and DONG Energy A/S for making data from the Horns Rev offshore wind farm available for the investigation.

## 7. References

- [1] Hansen KS et al. (2012); *Park power deficit due to atmospheric stability*. Presented at the Science of making Torque from Wind conference in Oldenburg, October 9-11, 2012.
- [2] Schmidt B et al. (2011); *Load validation and comparison versus certification approaches of the Risø Dynamic Wake Meandering model implementation in GH Bladed*, presented at EWEA2011, 14-17 March 2011, Brussels.
- [3] Larsen TJ et al. (2012); *Validation of the dynamic wake meander model for loads and power production in the Egmond aan Zee wind farm*. Wind Energy, we. 1563, 2012.
- [4] Hansen KS et al. (2013); *The impact of turbulence intensity and atmospheric stability on power deficits due to wind turbine wakes at Horns Rev wind farm*. Wind Energy, we. 512, 2011.
- [5] Bronstein A (2009); *Determination of Calibration Constants on Mill 14 at Horns Rev Offshore Wind Park*, DONG Energy A/S, May 2009 (confidential).
- [6] Johansen NA (2009); *Verification of simulated fatigue loads on wind turbines operating in wakes*. Report nr. MEK-FM-EP 2009-10, July 2009.
- [7] Barthelmie RJ, et al. (2011); *Flow and wakes in large wind farms: Final report for UpWind WP8, Appendix 6: Guideline to wind farm wake analysis*. Report number Risø-R-1765(EN).
- [8] Gryning, S-E, et al. (2007); *On the extension of the wind profile over homogeneous terrain beyond the surface layer*. Boundary-Layer Meteorology 124, 251-683.
- [9] Monin AS, Obukhov AM (1954); *Basic laws for turbulent mixing in the ground layer of the atmosphere*. Trans. Geophys. Inst. Akad.,Nauk USSR 151, 163-187
- [10] Sathe A, Gryning S-E, Penã A (2011); *Comparison of the atmospheric stability and wind profiles at two wind farm sites over a long marine fetch in the North Sea*. Wind Energy, we.456, 2011
- [11] Veldkamp HF (2006); *Chances in wind energy. A probabilistic approach to wind turbine fatigue design*, Ph.D. dissertation, TU-Delft.
- [12] Larsen GC, et al. (2008); *Wake meandering - a pragmatic approach*. Wind Energy, 11, 2008, pp. 377–395.